

Long-term regional trend and variability of mean sea level during the satellite altimetry era

Quang-Hung Luu^{1,2}, Qing Wu³, Pavel Tkalich⁴, Ge Chen^{3,5}

¹ Faculty of Science, Engineering and Technology, Swinburne University of Technology, Hawthorn, Victoria, 3122, Australia.

² School of Interdisciplinary Studies, Vietnam National University, Hanoi, Cau Giay, Hanoi, 10000, Vietnam. (Q-HL) (Corresponding author) E-mail: hluu@swin.edu.au. ORCID iD: <https://orcid.org/0000-0002-7771-9836>

³ Tropical Marine Science Institute, National University of Singapore, Kent Ridge, 119227, Singapore. (QW) E-mail: wuqingouc@gmail.com. ORCID iD: <https://orcid.org/0000-0001-7430-7169>

(GC) (Co-corresponding author) E-mail: gechen@ouc.edu.cn. ORCID iD: <https://orcid.org/0000-0003-4868-5179>

⁴ College of Information Science and Engineering, Ocean University of China, Qingdao, Shandong, 266100, China. (PT) E-mail: tmspt@nus.edu.sg. ORCID iD: <https://orcid.org/0000-0001-7527-0740>

⁵ Laboratory for Regional Oceanography and Numerical Modeling, Qingdao National Laboratory for Marine Science and Technology, Qingdao, Shandong, 266100, China.

Summary: The rise and fall of mean sea level are non-uniform around the global oceans. Their long-term regional trend and variability are intimately linked to the fluctuations and changes in the climate system. In this study, geographical patterns of sea level change derived from altimetric data over the period 1993-2015 were partitioned into large-scale oscillations allied with prevailing climatic factors after an empirical orthogonal function analysis. Taking into account the El Niño–Southern Oscillation (ENSO) and the Pacific Decadal Oscillations (PDO), the sea level change deduced from the multiple regression showed a better estimate than the simple linear regression thanks to significantly larger coefficients of determination and narrower confidence intervals. Regional patterns associated with climatic factors varied greatly in different basins, notably in the eastern and western regions of the Pacific Ocean. The PDO exhibited a stronger impact on long-term spatial change in mean sea level than the ENSO in various parts of the Indian and Pacific Oceans, as well as of the subtropics and along the equator. Further improvements in the signal decomposition technique and physical understanding of the climate system are needed to better attain the signature of climatic factors on regional mean sea level.

Keywords: regional sea level trend; sea level rise; climate variability; El Niño-Southern Oscillation; Pacific Decadal Oscillations.

Tendencia regional a largo plazo y variabilidad del nivel medio del mar en la era de la altimetría por satélite

Resumen: El aumento y la reducción del nivel medio del mar en los océanos del planeta no son valores uniformes. Su comportamiento a largo plazo y su variabilidad están íntimamente ligados a las fluctuaciones y cambios de los sistemas climáticos. En este estudio, los patrones de cambio del nivel del mar, derivados de datos altimétricos obtenidos en el periodo de 1993 a 2015, se dividieron en oscilaciones a gran escala y se compararon con factores climáticos prevalentes obtenidos de un análisis de Función Ortogonal Empírica. Cuando se toman en cuenta la Oscilación Sur de El Niño (ENSO) y las Oscilaciones Decenales del Pacífico (PDO), el cambio del nivel del mar deducido de una regresión múltiple produce mejores estimaciones que una regresión lineal simple al tener coeficientes de determinación con un valor más grande e intervalos de confianza con valores más estrechos. Los patrones regionales asociados con los factores climáticos variaron considerablemente para diferentes cuencas, notablemente en las regiones orientales y occidentales del océano Pacífico. Se observa que las PDO mostraron un impacto más importante en el cambio espacial a largo plazo de la media del nivel del mar que la ENSO en varias partes de los océanos Índico y Pacífico, al igual que en las regiones subtropicales y alrededor de la línea del Ecuador. Se necesitan mayores mejoras en las técnicas de descomposición de señales y entendimiento físico de los sistemas climáticos para representar más precisamente la influencia de los factores climáticos en la media del nivel regional del mar.

Palabras clave: tendencia regional del nivel del mar; subida del nivel del mar; variabilidad climática; Oscilación Sur de El Niño (ENSO); Oscilaciones Decenales del Pacífico (PDO).

Citation/Como citar este artículo: Luu Q.-H., Wu Q., Tkalich P., Chen G. 2019. Long-term regional trend and variability of mean sea level during the satellite altimetry era. *Sci. Mar.* 83(2): 111-120. <https://doi.org/10.3989/scimar.04691.05A>

Editor: A. Alvera.

Received: July 19, 2017. **Accepted:** March 28, 2019, **Published:** May 17, 2019.

Copyright: © 2019 CSIC. This is an open-access article distributed under the terms of the Creative Commons Attribution 4.0 International (CC BY 4.0) License.

INTRODUCTION

The global mean sea level (MSL) has been rising since the beginning of the twentieth century (IPCC 2013) and more rapidly during the last 20 years (Chen et al. 2017). Quantifying the rate and patterns of MSL change is of great importance (Jevrejeva et al. 2009, Marcos and Amores 2014, Luu et al. 2018) but is still challenging (Hay et al. 2015), mostly due to uncertainty in the measurement (Cazenave et al. 2014, Bos et al. 2014, Dieng et al. 2017) and interpretation (Visser et al. 2015, Dangendorf et al. 2017, Royston et al. 2018) of sea level data. Dating back to the eighteenth century, tide gauge records have long been a source of the spatio-temporal rates of MSL change. However, their limitations are sparseness, uneven geographic distribution, high sensitivity to local geodynamic and hydrological influences and, notably, unavailability in the open oceans. The launch of oceanographic satellites since 1993 provided an unprecedented opportunity to reveal the spatial patterns of sea level change with global coverage, capturing the non-uniformity in trend and variability (Ablain et al. 2015, 2017, Nerem et al. 2018).

In some regions of the western tropical Pacific Ocean, the MSL change rate has been shown to be 3 to 4 times higher than the global rate for the period 1993-2011, thanks to the exploitation of altimetric data (Zhang and Church 2012, Frankcombe et al. 2015). Regional change of MSL results from a complicated combination of several climatic factors at different timescales and geographical distributions (Hughes and Williams 2010, Stammer et al. 2013, Chen et al. 2018). The El Niño Southern Oscillation (ENSO) is a major global driver of interannual sea level variability, being prominent in the Pacific Ocean and the Indian Ocean (Landerer et al. 2008, Chen et al. 2010, Boening et al. 2012), which during some extreme events show a local rise in level of approximately 30 cm (Becker et al. 2012, McGregor et al. 2012, Widlansky et al. 2014). The Pacific Decadal Oscillations (PDO) also affect sea level variability, especially in the North Pacific region, where this climate fluctuation could modulate the sea level by 10 cm in some regions (Hamlington et al. 2013, Luu and Tkalich 2014, Frankcombe et al. 2015). Qualifying the regional MSL change may also have an alternative social implication, such as determining land areas subject to a sovereignty claim in the South China Sea (Lyons et al. 2018).

While many efforts have been made to derive the globally averaged MSL rise rate linked to global warming (e.g. Dangendorf et al. 2015, Slagen et al. 2016, Wu et al. 2017), its regional patterns have received less attention. The separation of regional trend and variability required a sufficiently long period for two reasons. Firstly, climate oscillations may increase the MSL by 50 mm or higher within a year, which was significantly greater than the annual increase (<5 mm) linked to global warming (Han et al. 2010, Tkalich et al. 2013, Luu et al. 2015). Secondly, each climate factor has a different spatial impact on the Earth's oceans. Many works (Zhang and Church 2012, Palanisamy et

al. 2015) attribute a large part (>12 mm year⁻¹) of the MSL rise observed in the western tropical Pacific to climate variability. In a recent analysis using climate model ensembles, Fasullo and Nerem (2018) showed that climate forcing associated with the ENSO and the PDO contribute significantly to the spatial patterns of global MSL rise.

In this study, we extend the work of Zhang and Church (2012) using satellite altimetry data in three aspects. First, our domain consists of not only the Pacific Ocean, but also the Indian and Atlantic oceans. Second, we took four dominant modes of sea level variability into consideration instead of two modes, accompanied by a better statistical model to correct for autocorrelation. Lastly, we further considered the lagged times to represent the delayed response of climate impact on sea level.

DATA AND METHOD

Monthly sea level data from the Ssalto/Duacs delay-time product provided by the Archiving, Validation and Interpretation of Satellite Oceanographic Data service (AVISO, <http://www.aviso.altimetry.fr/en/data.html>) for the period 1993-2015 were obtained. The product was reconstructed from ten satellite missions having fine spatial bins and delivering data at a grid resolution of 1/4°×1/4°. We removed the seasonal cycle, applied a 5-month moving average for time series and smoothed spatial patterns to a resolution of 1°×1° covering the domain 0-360°, 50°S-60°N. To correlate with climate fluctuations, we decomposed the time series of sea level at each grid point into decadal and interannual components, as suggested by previous studies (Vimont 2005, Zhang and Church 2012). The decadal dataset was obtained by applying 25-month moving averages followed by another 37-month smoothing on the original time series at each grid point, while the interannual dataset was achieved by subtracting the decadal components from the time series, as suggested by Zhang and Church (2012). For discussion, we further used the sea level data provided by the Commonwealth Scientific and Industrial Research Organization (CSIRO), which combined data from four satellite measurements TOPEX/Poseidon, Jason-1, Jason-2/OSTM and Jason-3, available from http://www.cmar.csiro.au/sealevel/sl_data_cmar.html).

We used different climate indices to associate with dominant modes of sea level variability. The highest correlated forcings are the ENSO, the Central Pacific ENSO (CP ENSO) and the PDO. The multivariate ENSO index (MEI; <http://www.esrl.noaa.gov/psd/enso/mei/>) was chosen as a proxy of the ENSO (Wolter and Timlin 1998) that has a strong correlation with interannual changes in sea level (Luu et al. 2015, Wu et al. 2017). The PDO index was adopted (from <http://research.jisao.washington.edu/pdo/>) alongside CP ENSO, as an alternative climate factor akin to the ENSO (Kao and Yu 2009, available at <http://www.ess.uci.edu/~yu/2OSC/>). The solar radiation data used by Luu et al. (2018) are not considered in this study.

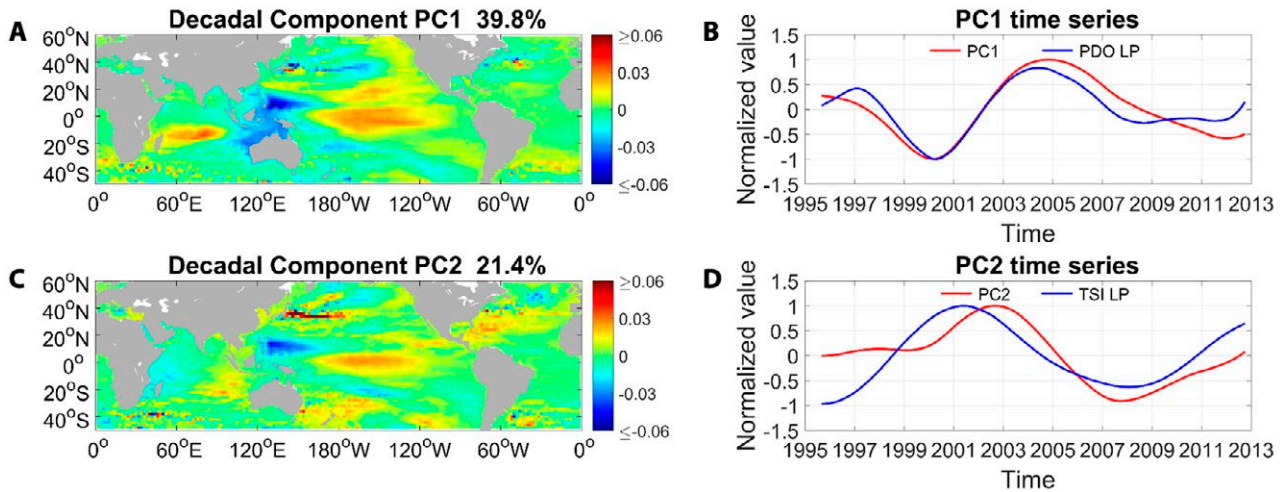


Fig. 1. – Spatial patterns of the first dominant mode EOF1 (A) and its corresponding (normalized) time-series t_{EOF1} (B) computed from the de-trended 5-month running mean of decadal component of AVISO sea level data for the period 1993–2012. De-trended low-pass-filtered indices of the PDO are added in subplot B.

To ease the autocorrelation problem arising from the original least square fitting, the first-order autoregressive and first-order moving average (ARMA(1, 1)) was applied instead of the commonly used first-order autoregressive (AR(1)) model. As pointed out by Foster and Brown (2015), its advantage over the AR(1) model is its capability to resolve the underestimation of standard errors. All statistical values in our study were computed for a two-tailed Student t-test at a 95% significance interval. Note that the corrected confidence intervals are associated with smoothed data and might consist of unavoidable dominant uncertainties, including observational errors in the satellite orbit corrections applied (Ablain et al. 2015).

MODES OF SEA LEVEL VARIABILITY

The empirical orthogonal functions (EOF) technique has been applied successfully in various climate studies (e.g. Bjornsson and Venegas 1997, Church and White 2011). Its advantage is its ability to decompose the spatio-temporal signals into dominant modes associated with spatial patterns and time series by means of orthogonal basis functions. We used the PCAtool developed in Matlab software by Guillaume Maze (given at <https://au.mathworks.com/matlabcentral/fileexchange/17915-pcatool>) to implement a regular (non-rotating) EOF analysis on sea level variability. Four dominant modes were detected from this analysis: the leading mode from decadal time series and three modes from interannual signals. They were then associated with well-identified climatic drivers that have high correlations, as described below.

For the decadal dataset, the first three leading EOF modes explained 61.2% of total variance. Accounting for 39.8% of the signals, the most dominant mode (EOF1-D) exhibited seesaw patterns in the Pacific Ocean extending symmetrically to mid-latitudes, and in the Indian Ocean (Fig. 1A). Positive values were observed in the eastern Pacific region (180–100°W; 15°S–20°N) and the western Indian Ocean (50–90°E;

0–20°S), while negative values were observed near the western Pacific-eastern Indian areas (110–150°E; 20°S–20°N) and in the central North Pacific (160°E–140°W; 20–40°N). Its temporal evolution was highly correlated (Pearson’s correlation coefficient, $r=0.92$) with the fluctuations of the low-pass-filtered PDO index (Fig. 1B). We attributed this mode to the PDO, which was consistent with previous findings (Zhang and Church 2012, Frankcombe et al. 2015).

Three leading modes revealed from the interannual dataset explained 39.9% of total variance. The largest principal mode (EOF1-I) accounted for 26.8% of net signals and was related to the ENSO influence due to a significant correlation ($r=0.94$) between spatio-temporal patterns of this mode and the high-pass-filtered ENSO index (Fig. 2B). For example, in the Pacific Ocean, a narrow seesaw pattern was found, comprising a negative anomaly in the west of the tropical equator (120–170°E; 5°S–15°N) and a positive anomaly extending from the middle of the Pacific toward the western coast of the American continent (180–65°W; 10°S–10°N). The results were similar to the ENSO-induced sea level in the tropical Pacific Ocean revealed in other studies (e.g. Hamlington et al. 2011, Widlansky et al. 2014). In contrast, a high anomaly was depicted around the western part of the Indian Ocean (40–100°E; 10°S–10°N), while a negative one was detected in its eastern part. These patterns were linked to the ENSO in earlier studies (Hamlington et al. 2011, Zhang and Church 2012).

The second principal mode (EOF2-I) showed a smaller contribution to the interannual variance (8.8%) and had a complicated structure. In the Pacific, it comprised a narrow negative equatorial belt bounded between 5°S and 5°N, a positive bar mirrored over the latitudinal line of 10°N, and a significantly negative trace appearing in the South Pacific Convergence Zone (SPCZ). Adoption of the MEI yielded the best correlation of 0.90 for a 7-month lag (Fig. 2D). This half-year lag was consistent with the findings of Widlansky et al. (2014), who observed an interaction between sea

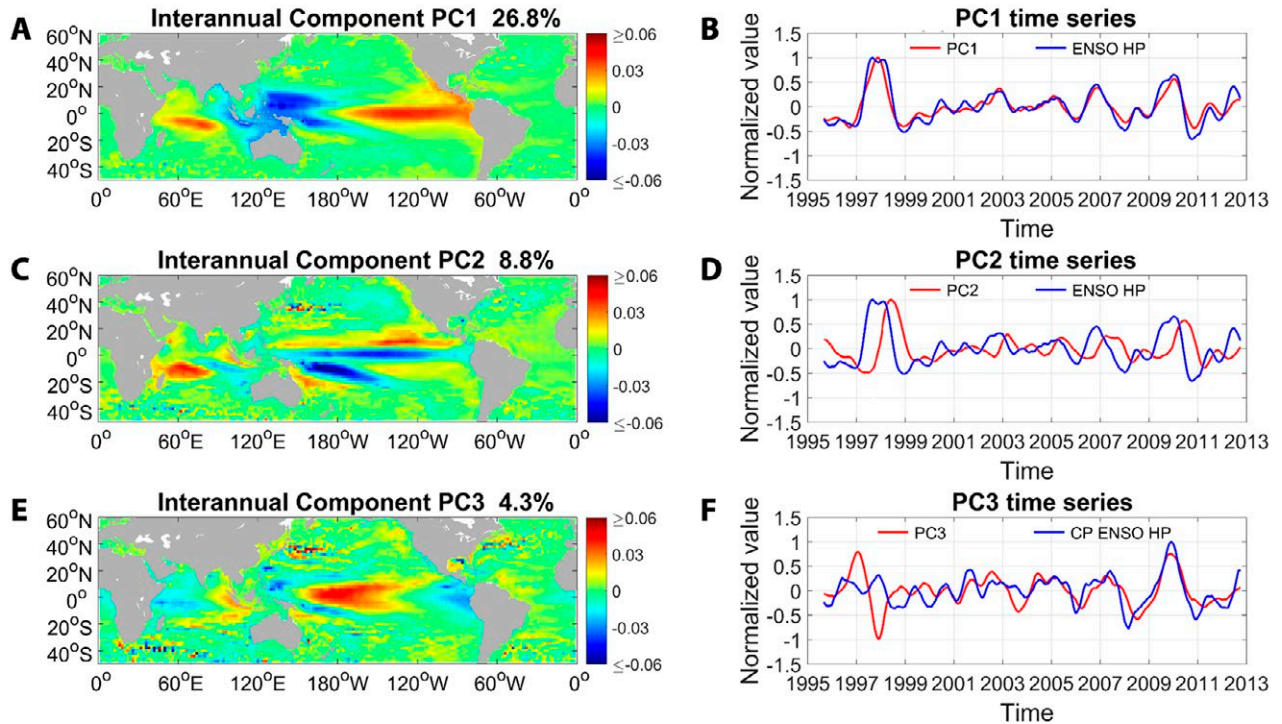


Fig. 2. – Same as Figure 1, except that the EOF analysis is applied for interannual variability. The de-trended ENSO high-pass-filtered index is appended in subplots B and D, and the de-trended CP ENSO high-pass-filtered index is inserted in subplot F for comparison. In addition, the approximated index for EOF2 is also plotted in subplot D

level in the northwest and southwest Pacific tropical regions and the ENSO extreme events. Meanwhile, the third principal mode (EOF3-I) depicted a strong positive anomaly in the Niño-4 region (5°S-5°N, 160°E-150°W) shown in Fig. 2E. This anomaly was previously reported by Kug et al. (2009), who pointed to the CP ENSO influence. The highest correlation between the temporal evolution of the CP ENSO and the mode was 0.56 after a 2-month lag (Fig. 2F and Table 1), contributing 4.3% to total variance.

The time lags between climate indices and principal modes of sea level variability are summarized in Table 1. To further examine the sensitivity of these time lags, we repeated the EOF analysis on the sea level dataset provided by CSIRO and obtained similar results (Table 1).

REGRESSION ANALYSIS

Regression models

In the simple model, the sea level change rate was derived from a single-value linear regression (SVLR) analysis. At a given geographic location (x,y), the geo-

centric sea level $H(x,y,t)$ with respect to its long-term mean at the given time t is described by the equation:

$$H(x,y,t) = s_{SVLR}(x,y)t + c_{SVLR}(x,y) \tag{1}$$

where s_{SVLR} is the linear rate of sea level rate over the considered period, and c_{SVLR} is a constant in the SVLR analysis. By calculating the rates at different geographic locations, we established a global map showing rates of sea level change during the given period (Fig. 3A). The analysis was carried out on the monthly time-series from each of 360×180 grid points.

In the second model, we further considered more variables in the equation using multiple linear regression (MVLr) analysis. These variables were defined from above dominant climate indices, which have been shown in the EOF analysis to have high correlations with the sea level. Table 1 presents definitions of the Interannual Climate Indices (ICIs) and the Decadal Climate Indices (DCIs) based on the MEI, the CP ENSO and the PDO. Using the defined climate indices, we estimated the linear rate of change (s_{MVLr}) from the equation

Table 1. – Defined climate indices derived from filtering original climate indices in different datasets and their corresponding time differences (months).

Sources	Original index Filter applied Defined index Coverage	MEI High-pass ICI1 Lagged time (months) of defined index in comparison with original index	MEI High-pass ICI2	CP ENSO High-pass ICI3	PDO Low-pass DCI1
CSIRO (1993-2011) (Zhang and Church 2012)	Pacific Ocean	0	-	-	0
AVISO (1993-2015) (This study)	Global oceans	0	7	2	0
CSIRO (1993-2015) (This study)	Global oceans	0	7	3	0

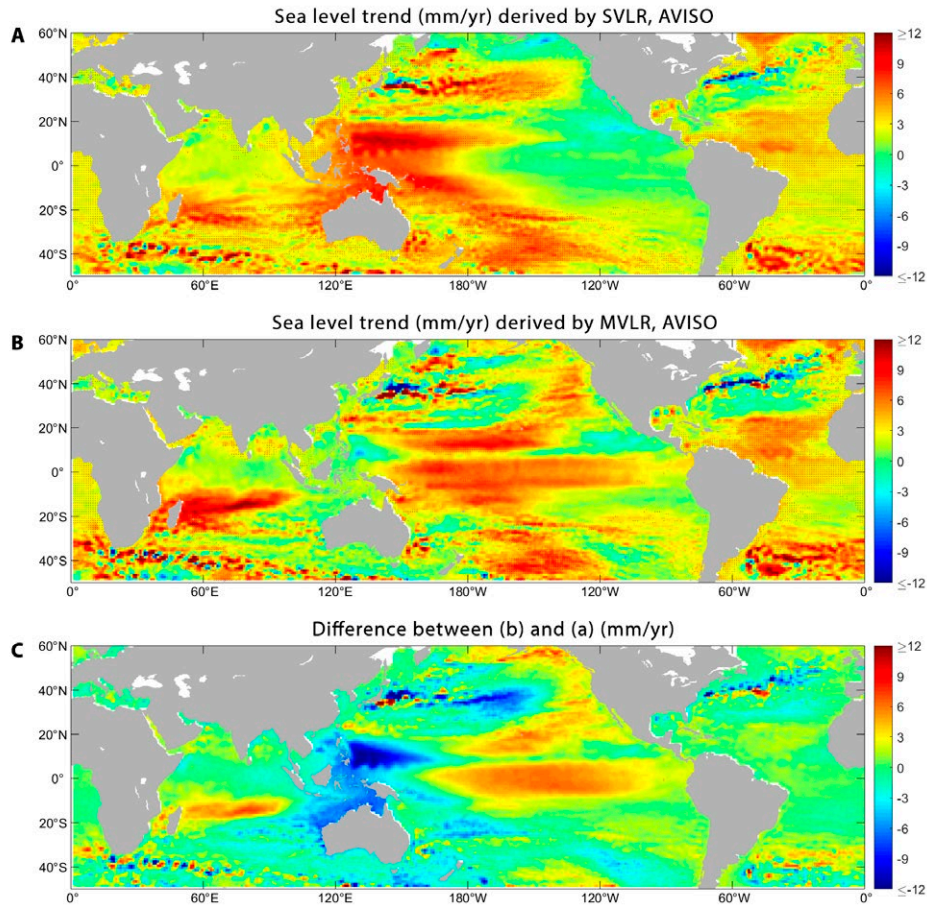


Fig. 3. – Regional patterns of sea level change rates derived from AVISO data using (A) SVLR, (B) MVLR and (C) trend aliasing due to interannual and decadal variabilities for the period 1993-2012. Stippling indicates a trend exceeding the 95% confidence level.

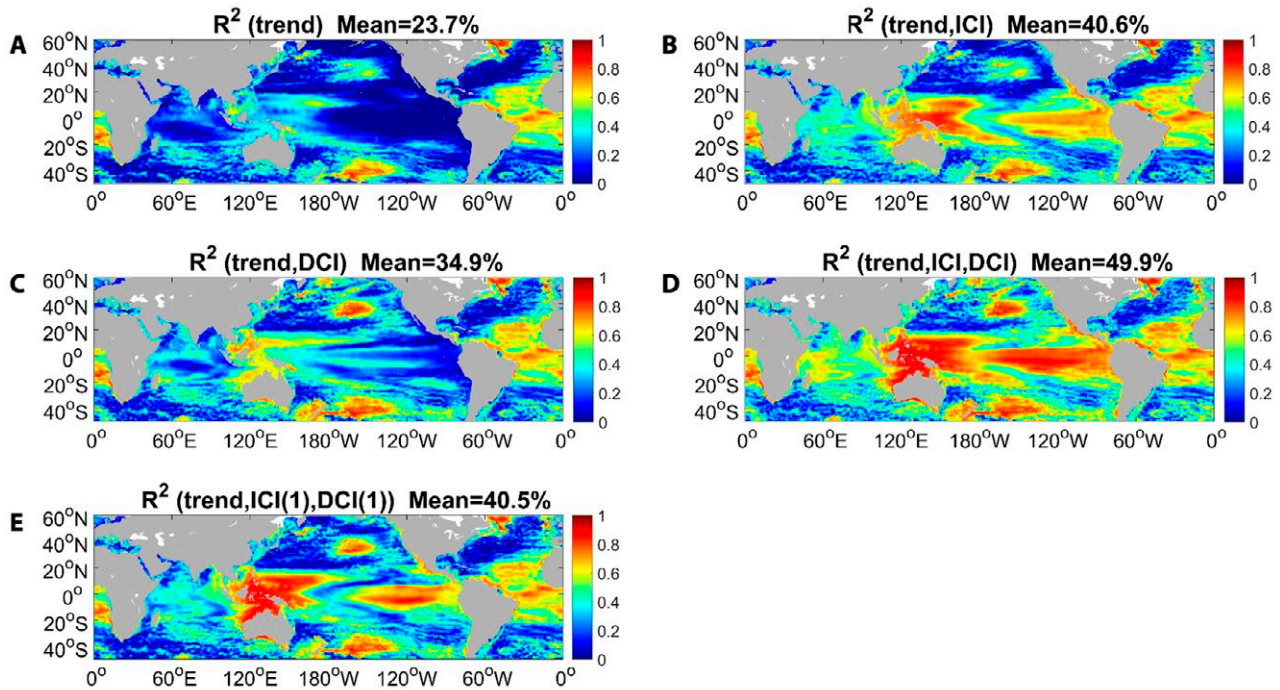


Fig. 4. – The coefficients of determination measuring the goodness of fit computed from the AVISO data for the period 1993-2012 using the following models: A, SVLR; B, MVLR without DCIs; C, MVLR with only trend and DCIs; D, MVLR with respect to trend along with all the dominant ICIs and DCIs.

Table 2. – Percentage of explained covariance in regression models (SVLR and MVLR with two dominant modes, and MVLR with all four dominant modes) using different datasets.

Sources	Global mean			Pacific Ocean			Indian Ocean			Atlantic Ocean		
	SVLR	MVLR 2 modes	MVLR 4 modes	SVLR	MVLR 2 modes	MVLR 4 modes	SVLR	MVLR 2 modes	MVLR 4 modes	SVLR	MVLR 2 modes	MVLR 4 modes
CSIRO (1993-2011)	-	-	-	23%	60%	-	-	-	-	-	-	-
Zhang and Church (2012)												
AVISO (1993-2015)	24%	41%	47%	21%	44%	51%	21%	36%	41%	35%	39%	42%
This study												
CSIRO (1993-2015)	31%	49%	53%	23%	49%	53%	35%	51%	56%	42%	47%	51%
This study												

$$H(x,y,t) = s_{\text{MVLR}}(x,y)t + c_{\text{MVLR}}(x,y) + i_1(x,y)\text{ICI1} + i_2(x,y)\text{ICI2} + i_3(x,y)\text{ICI3} + d_1(x,y)\text{DCI1} \quad (2)$$

where $s_{\text{SVLR}}(x,y)$ is the sea level rise rate; $i_k(x,y)$ ($k=1, 2, 3$) and $d_k(x,y)$ ($k=1$) are the coefficients representing the contributions from ICIs and DCIs; and $c_{\text{SVLR}}(x,y)$ is a constant.

Model performance and contribution of climate factors

We used the coefficient of determination (R^2) to measure the goodness-of-fit of the models. It is computed as a percentage from the ratio of explained variance (derived from the regression model) to total variance, resulting in a value between 0% and 100%. Table 2 and Figure 4 show the coefficients computed from the regression models: SVLR, MVLR with two dominant modes, and MVLR with four dominant modes.

For the AVISO dataset, the SVLR model explained 24% of the globally averaged variance. The use of the MVLR model with all dominant modes significantly doubled the R^2 to 47% (Table 2). The MVLR model provides better results than the SVLR in the Pacific Ocean, where the goodness-of-fit difference was almost three-fold. The variance in the Atlantic Ocean was well explained by the SVLR (35%), in which the involvement of four additional variables enhanced the estimates by only 7%. A similar success of the MVLR over the SVLR was observed in the CSIRO dataset (Table 2).

Figure 4 depicts relative influences of the dominant ICI and DCI modes in the MVLR models for the AVISO dataset. The coefficient of determination in the MVLR model using the ICIs was 41%, which is 6% higher than that of the DCIs. This means that the contribution of the interannual indices was greater than that of the decadal components in the overall MVLR model. When both ICIs and DCIs were included in the regression (Fig. 4D), the R^2 ratio was the highest among the MVLR models considered, reaching 50%. Notable improvements are observed in the tropical Pacific Ocean and part of the mid-latitude regions ($R^2 > 80\%$). In the Pacific Ocean, ICIs dominated the regional variance. In the Atlantic Ocean, the two indices were equally important in contributing to total variance.

The best model depicting the rates of regional sea level rise is MVLR using the dominant modes of both the ICIs and the DCIs (Fig. 5), which was used to derive the characteristics of regional sea level rise rates to be discussed in the next section.

REGIONAL SEA LEVEL CHANGE

Spatial patterns of sea level change

Figure 3A displays the observed patterns of sea level rise in global oceans for the period 1993-2012. The rate was high ($>10 \text{ mm year}^{-1}$) in the western areas of the Pacific Ocean, whereas a marginal decreasing rate was seen in the eastern areas. In contrast, the increasing tendency was observed in the Indian and Atlantic oceans, except for a few small regions at high latitude.

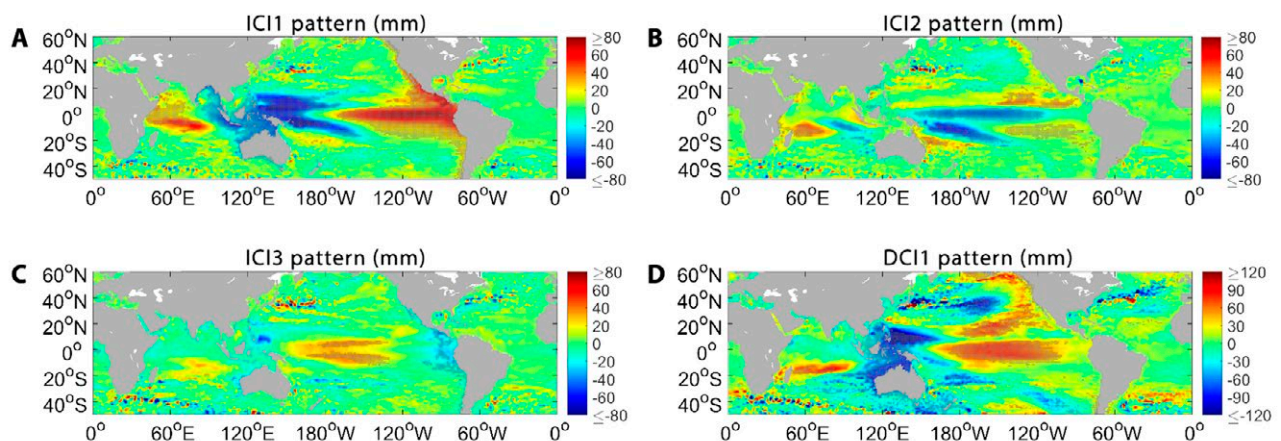


Fig. 5. – Patterns of ICIs and DCIs derived from the corresponding coefficients in MVLR: A, ICI1; B, ICI2; C, ICI3; and D, DCI1 for the same dataset. Stippling indicates a trend exceeding the 95% confidence level.

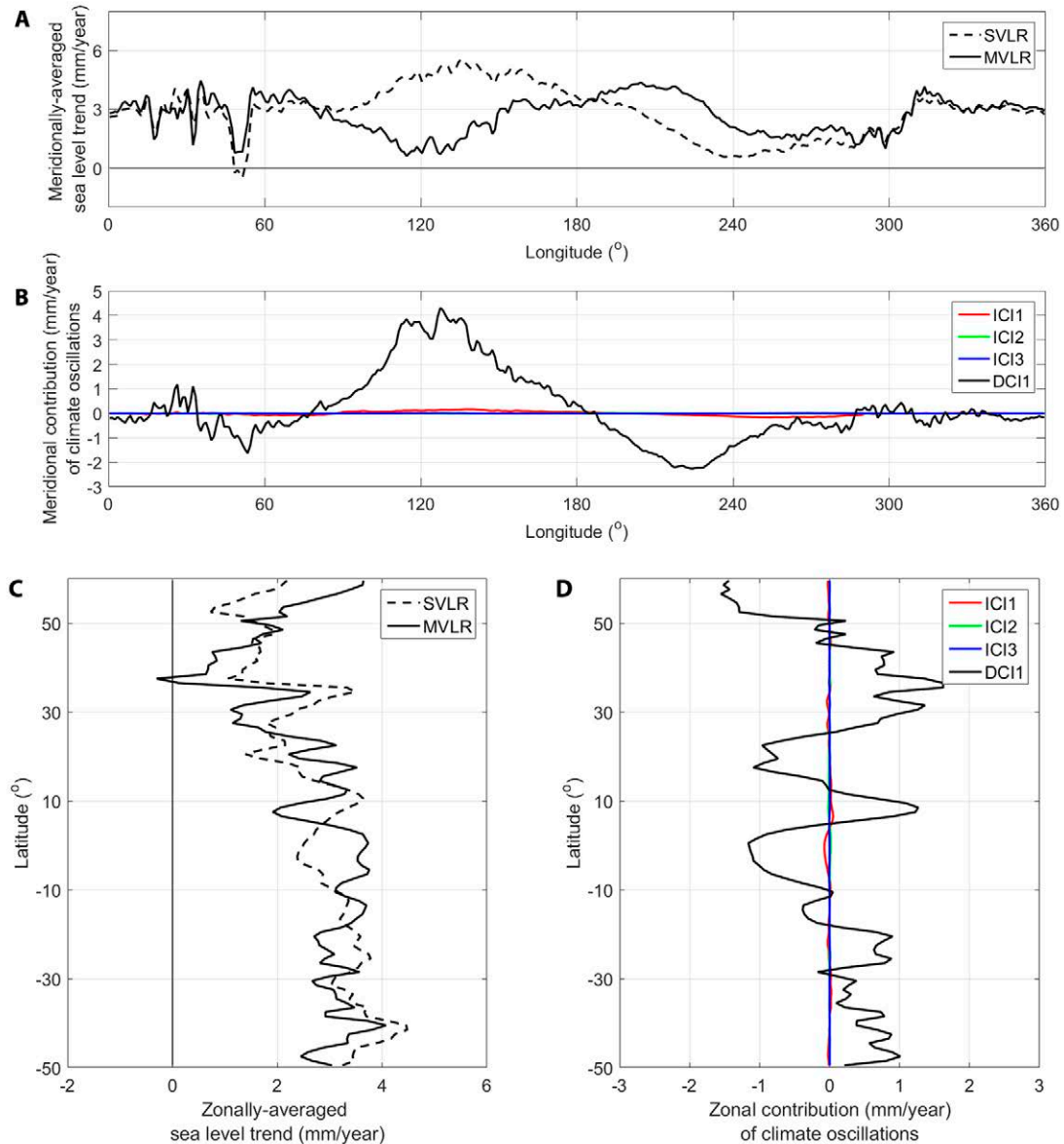


Fig. 6. –Meridional (A) and zonal (C) averaged patterns of sea level rise derived from AVISO data over the period 1993–2012 using regressions (SVLR and MVLR). Contributions from climate oscillations are depicted as functions of longitude (B) and latitude (D).

In overall, the highest rates ($>6 \text{ mm year}^{-1}$) were found in the tropical regions ($40\text{--}120^\circ\text{E}$; $10\text{--}30^\circ\text{S}$) and at mid-latitudes (around 40°S) in the Indian Ocean and tropical Pacific ($150^\circ\text{E}\text{--}125^\circ\text{W}$; $20^\circ\text{S}\text{--}20^\circ\text{N}$). However, these high rates failed to pass the significance test, implying that the SVLR model did not explain changes in sea level well.

The regional rate after the MVLR analysis is displayed in Figure 3B. A significant adjustment was noted in the Pacific Ocean. The positive change in sea level ($>10 \text{ mm year}^{-1}$) shifted from its western basin to the tropical areas ($150^\circ\text{E}\text{--}125^\circ\text{W}$; $20^\circ\text{S}\text{--}20^\circ\text{N}$), with weakened extremes. The rise became stronger in some areas of the Indian Ocean (around 15°S) and the Atlantic tropics ($0\text{--}60^\circ\text{W}$; $0\text{--}20^\circ\text{N}$). The areas with a negative rate in the eastern Pacific were diminished.

In comparison, the aliasing (Fig. 3C) was defined by subtracting the MVLR regional rate (Fig. 3B) from

the SVLR one (Fig. 3A), which demonstrated the influence of climate variability on the regional rate of sea level change. The largest deviations ($>9 \text{ mm year}^{-1}$) in aliasing were found in the Indo-Pacific tropics. The aliasing was unlikely to have been caused by the ICIs because no noticeable rates were observed in their indices. Instead, it was mainly attributed to decadal variability.

Meridional and zonal change in sea level

To further examine the spatial variability, sea level change rates were averaged in the meridional (Fig. 6A) and zonal (Fig. 6C) directions. In the meridional axis, the largest discrepancy was observed in the region between 90°E and 100°W , which includes mainly the Pacific Ocean. When the pattern was compared with the climate factors averaged over the entire available

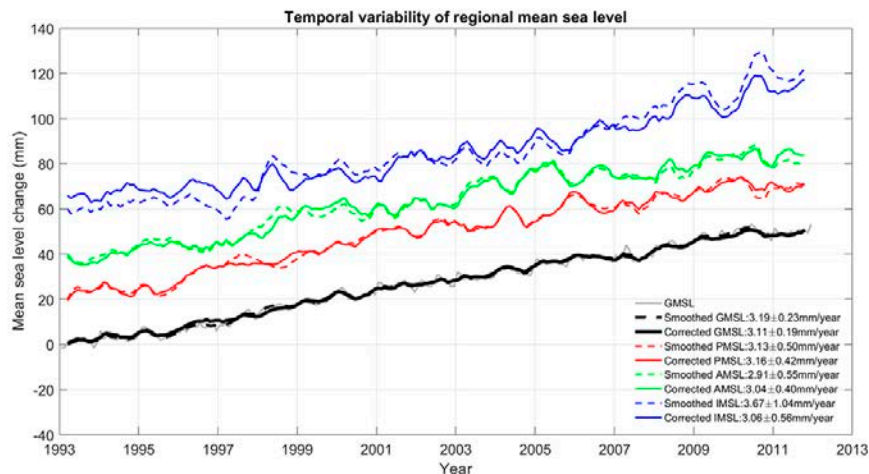


Fig. 7. – Time-series of temporal mean sea level change derived from AVISO data from 1993 to 2012 in the global averaged oceans (GMSL, black), Pacific Ocean (PMSL, red), Atlantic Ocean (AMSL, green) and Indian Ocean (IMSL, blue).

latitudinal range (Fig. 6B), it was apparent that the contribution probably resulted from the PDO. Meanwhile, meridional distribution of the aliasing in the Indian Ocean and the Atlantic Ocean was smaller.

In the zonal axis, the MSL rose faster in the Southern Hemisphere than in the Northern Hemisphere (Fig. 6C). Along the equator (between 10°S and 10°N), the MSL rose at a rate of about 3.5 mm year⁻¹, which was 1.0 mm year⁻¹ higher than estimated in the SVLR model (Fig. 6C). The PDO was also responsible for the high rate in latitudinal regions covering the subtropics (30 to 50°S and 30 to 50°N). The zonal influence of interannual components was negligible for the long-term trend (Fig. 6D).

Temporal variability of mean sea level

Time series of the MSL change are depicted in Figure 7A. The main finding is that, while the sea level rise rates over the period 1993–2012 were slightly altered, their corresponding 95% confidence intervals were narrowed significantly. In the Pacific and Atlantic Oceans, the rates for the same episode were marginally higher (by 3–4%), with the confidence bands narrowed by 16 to 27%. The noticeable change was in the Indian Ocean, where the rate was 20% higher than for the simple linear regression, accompanied by a better (i.e. narrower) estimation of confidence band of 0.56 mm year⁻¹, which was 46% smaller.

To examine the role of each climatic factor, we removed the index from the multiple linear regression (Eq. 2) and computed the contribution as the sea level difference between the modified and original MVL models (Fig. 7B). It was found that the ENSO exhibited a prevailing impact in year-to-year sea level changes in all oceanic basins, causing the greatest interannual variability. The influence of the PDO (i.e. DCI1) was the strongest, and probably caused an alteration of the apparent sea level rise in the Indian Ocean. Although the contribution of the CP ENSO (ICI2) was insignificant in the long term, it had a noticeable impact on the interannual scale, for instance, over the period 1997–1998.

CONCLUSION AND DISCUSSION

Regional changes in sea level over a 20-year period were partitioned by taking advantage of high-resolution satellite altimeter data. To determine the components of sea level variability, its dominant modes were identified from interannual and decadal time series by means of an EOF method, which linked three leading interannual modes to the ENSO and the CP ENSO, and the principal decadal mode to the PDO. MVL models were used to separate the trend and variability, which showed an improvement versus the SVLR in two statistical measures. Firstly, the use of the multivariate model improved the coefficients of determination for two datasets used, namely AVISO and CSIRO. Secondly, the MVL model also significantly eased the statistical uncertainty in estimating the sea level change rate. The MVL model was then employed to display the patterns and temporal variability of regional sea level change.

Significant adjustments were visible in the Pacific Ocean, where the positive change in sea level (>10 mm year⁻¹) shifted from its western basin to the tropical areas (150°E–125°W; 20°S–20°N), while the negative rate on its eastern side diminished. The rise became stronger in some areas of the Indian Ocean (around 15°S) and Atlantic tropics (0–60°W; 0–20°N). Along the meridional axis, the largest discrepancy was observed in the Pacific Ocean, which is mainly contributed by the PDO. The MSL rose faster in the Southern Hemisphere than in the Northern Hemisphere. In the temporal change, the ENSO exhibited prevailing impacts in interannual sea level variations in all oceanic basins. Despite being insignificant in the long term, the CP ENSO made a noticeable contribution at the interannual scale, for instance, over the period 1997–1998.

We derived the regional patterns of sea level change by means of a statistical approach using satellite data. Our results are consistent with the conclusion from a recent study by Fasullo and Nerem (2018), who used climate model ensembles and came to the similar conclusion that external climate forcing including the

ENSO and the PDO is probably a main contributor to the observed non-uniform patterns of sea level rise in the global oceans. They further suggested that these patterns might remain for decades, and will probably be intensified under the changing climate.

For future studies, the fairly low significant level in some regions and the small variances explained by interannual modes suggested that improvements are desirable. These may include the introduction of other climatic and non-climatic factors and a more suitable regression model, as there are still a lot of interannual and decadal variabilities left after applying the MVL model, which alias into the trend estimates. In fact, this is a great challenge, since a quantitative relationship between regional sea level change and climate fluctuations is undeterminable outside the context of the Earth's sophisticated climate system, which is driven by both deterministic and stochastic processes. As a result, further continuing efforts are needed to give deeper insights into not only the statistical decomposition technique to attain the rate, but also the establishment of non-deterministic mathematical relationships between sea level variability and other physical components of the climate system, including ice sheet melts and volcano eruptions (Slangen et al. 2016, Marcos et al. 2017, Huang et al. 2018).

ACKNOWLEDGEMENTS

Chen G. and Wu Q. were jointly supported by the Natural Science Foundation of China under Grant Nos. 41331172, U1406404 and 61361136001, and by the National Laboratory for Marine Science and Technology under the Outstanding Scientist Project of the Ao-Shan Talents Programme (No. 2015ASTP-OS15). The analysis was conducted using the PCAtool developed by Guillaume Maze. The authors acknowledge the careful review and constructive comments from Prof. D. Vaqu e, Dr. A. Alvera, Dr T. Frederikse and anonymous reviewer(s). We thank Prof. S.P.H. Ng, Dr M.F. Lau and Prof. P.H.H. Then for providing computational facilities. Thanks are extended to V.M. Alb niz, A. Lounds and the Scientia Marina editorial office for the support with submission, and F.A.A. Freddy and T.N. Nguyen for their help with the Spanish translation.

REFERENCES

- Ablain M., Cazenave A., Larnicol G., et al. 2015. Improved sea level record over the satellite altimetry era (1993-2010) from the Climate Change Initiative project. *Ocean Sci.* 11: 67-82. <https://doi.org/10.5194/os-11-67-2015>
- Ablain M., Legeais J.F., Prandi P., et al. 2017. Satellite altimetry-based sea level at global and regional scales. *Surv. Geophys.* 38: 7-31. <https://doi.org/10.1007/s10712-016-9389-8>
- Becker M., Meyssignac B., Letetrel C., et al. 2012. Sea level variations at tropical Pacific islands since 1950. *Glob. Planet. Change* 80: 85-98. <https://doi.org/10.1016/j.gloplacha.2011.09.004>
- Bjornsson H., Venegas S.A. 1997. A manual for EOF and SVD analyses of climatic data, McGill University, 53 pp.
- Boening C., Willis J.K., Landerer F.W. et al. 2012. The 2011 La Ni a: So strong, the oceans fell. *Geophys. Res. Lett.* 39: L19602. <https://doi.org/10.1029/2012GL053055>
- Bos M.S., Williams S.D.P., Araujo I.B., et al. 2014. The effect of temporal correlated noise on the sea level rate and acceleration uncertainty. *Geophys. J. Int.* 196: 1423-1430. <https://doi.org/10.1093/gji/ggt481>
- Cazenave A., Dieng H.B., Meyssignac B., et al. 2014. The rate of sea-level rise. *Nat. Clim. Change* 4: 358-361. <https://doi.org/10.1038/nclimate2159>
- Chen G., Wang Z., Qian C., et al. 2010. Seasonal-to-decadal modes of global sea level variability derived from merged altimeter data. *Remote Sens. Env.* 114: 2524-2535. <https://doi.org/10.1016/j.rse.2010.05.028>
- Chen G., Peng L., Ma C. 2018. Climatology and seasonality of upper ocean salinity: a three-dimensional view from argo floats. *Clim. Dyn.* 50: 2169-2182. <https://doi.org/10.1007/s00382-017-3742-6>
- Chen X., Zhang X., Church J.A., et al. 2017. The increasing rate of global mean sea-level rise during 1993-2014. *Nat. Clim. Change* 7: 492-495. <https://doi.org/10.1038/nclimate3325>
- Church J.A., White N.J. 2011. Sea-level rise from the late 19th to the early 21st century. *Surv. Geophys.* 32: 585-602. <https://doi.org/10.1007/s10712-011-9119-1>
- Dieng H.B., Cazenave A., Meyssignac B., et al. 2017. New estimate of the current rate of sea level rise from a sea level budget approach. *Geophys. Res. Lett.* 44: 3744-3751. <https://doi.org/10.1002/2017GL073308>
- Dangendorf S., Marcos M., Muller M., et al. 2015. Detecting anthropogenic footprints in sea level rise. *Nat. Comm.* 6: 7849. <https://doi.org/10.1038/ncomms8849>
- Dangendorf S., Marcos M., W ppelmann G., et al. 2017. Reassessment of 20th century global mean sea level rise. *Proc. Nat. Acad. Sci.* 114: 5946-5951. <https://doi.org/10.1073/pnas.1616007114>
- Fasullo J.T., Nerem R.S. 2018. Altimeter-era emergence of the patterns of forced sea-level rise in climate models and implications for the future. *Proc. Nat. Acad. Sci.* 115: 12944-12949. <https://doi.org/10.1073/pnas.1813233115>
- Foster G., Brown P.T. 2015. Time and tide: analysis of sea level time series. *Clim. Dyn.* 45: 291-308. <https://doi.org/10.1007/s00382-014-2224-3>
- Frankcombe L.M., McGregor S., England M.H. 2015. Robustness of the modes of Indo-Pacific sea level variability. *Clim. Dyn.* 45: 1281-1298. <https://doi.org/10.1007/s00382-014-2377-0>
- Hamlington B.D., Leben R.R., Nerem R.S., et al. 2011. Reconstructing sea level using cyclostationary empirical orthogonal functions. *J. Geophys. Res. Oceans* 116: C12015. <https://doi.org/10.1029/2011JC007529>
- Hamlington B.D., Leben R.R., Strassburg M.W., et al. 2013. Contribution of the Pacific Decadal Oscillation to global mean sea level trends. *Geophys. Res. Lett.* 40: 5171-5175. <https://doi.org/10.1002/grl.50950>
- Han W., Meehl G.A., Rajagopalan B., et al. 2010. Patterns of Indian Ocean sea-level change in a warming climate. *Nat. Geos.* 3: 546-550. <https://doi.org/10.1038/ngeo901>
- Hay C.C., Morrow E., Kopp R.E., et al. 2015. Probabilistic reanalysis of twentieth-century sea-level rise. *Nature* 517: 481-484. <https://doi.org/10.1038/nature14093>
- Huang J., Zhang X., Zhang Q., et al. 2018. Recently amplified arctic warming has contributed to a continual global warming trend. *Nat. Clim. Change* 7: 875-879. <https://doi.org/10.1038/s41558-017-0009-5>
- Hughes C.W., Williams S.D.P. 2010. The color of sea level: Importance of spatial variations in spectral shape for assessing the significance of trends. *J. Geophys. Res.* 115: C10048. <https://doi.org/10.1029/2010JC006102>
- Intergovernmental Panel on Climate Change (IPCC). 2013. *Climate Change 2013: The Physical Science Basis. Contribution of Working Group I to the Fifth Assessment Report of the Intergovernmental Panel on Climate Change.* Stocker T.F., Qin D., et al. (eds), Cambridge University Press, Cambridge, United Kingdom and New York, NY, USA. 1585 pp. <https://www.ipcc.ch/report/ar5/wg1/>
- Jevrejeva S., Grinsted A., Moore J.C. 2009. Anthropogenic forcing dominates sea level rise since 1850. *Geophys. Res. Lett.* 36: L20706. <https://doi.org/10.1029/2009GL040216>
- Kao H.Y., Yu J.Y. 2009. Contrasting eastern-Pacific and central-Pacific types of ENSO. *J. Clim.* 22: 615-632. <https://doi.org/10.1175/2008JCLI2309.1>

- Kug J.S., Jin F.F., An S.I. 2009. Two types of El Niño events: cold tongue El Niño and warm pool El Niño. *J. Clim.* 22: 1499-1515. <https://doi.org/10.1175/2008JCLI2624.1>
- Landerer F.W., Jungclauss J.H., Marotzke J. 2008. El Niño–Southern Oscillation signals in sea level, surface mass redistribution, and degree-two geoid coefficients. *J. Geophys. Res. Oceans* 113: C08014. <https://doi.org/10.1029/2008JC004767>
- Luu Q.H., Tkalich P. 2014. Reconstruction of gappy mean sea level data. *Ind. J. Geo-Mar. Sci.* 43: 1316-1321.
- Luu Q.H., Tkalich P., Tay T.W. 2015. Sea level trend and variability around Peninsular Malaysia. *Ocean. Sci.* 11: 617-628. <https://doi.org/10.5194/os-11-617-2015>
- Luu Q.H., Wu Q., Tkalich P. et al. 2018. Global mean sea level rise during the recent warming hiatus from satellite-based data. *Remote Sens. Lett.* 9: 497-506. <https://doi.org/10.1080/2150704X.2018.1437291>
- Lyons Y., Luu Q.H., Tkalich P. 2018. Determining high-tide features (or islands) in the South China Sea under Article 121(1): a legal and oceanography perspective. In: Jayakumar S., Koh T. et al. (eds), *The South China Sea Arbitration: The Legal Dimension*, Edward Elgar Publ., pp. 128-153. <https://doi.org/10.4337/9781788116275.00015>
- Marcos M., Amores A. 2014. Quantifying anthropogenic and natural contributions to thermosteric sea level rise. *Geophys. Res. Lett.* 41: 2502-2507. <https://doi.org/10.1002/2014GL059766>
- Marcos M., Marzeion B., Dangendorf S., et al. 2017. Internal variability versus anthropogenic forcing on sea level and its components. *Surv. Geophys.* 38: 329-348. <https://doi.org/10.1007/s10712-016-9373-3>
- McGregor S., Gupta A.S., England M.H. 2012. Constraining wind stress products with sea surface height observations and implications for Pacific Ocean sea level trend attribution. *J. Clim.* 25: 8164-8176. <https://doi.org/10.1175/JCLI-D-12-00105.1>
- Nerem R.S., Beckley B.D., Fasullo J.T., et al. 2018. Climate-change-driven accelerated sea-level rise detected in the altimeter era. *Proc. Nat. Acad. Sci.* 115: 2022-2025. <https://doi.org/10.1073/pnas.1717312115>
- Palanisamy H., Cazenave A., Delcroix T., et al. 2015. Spatial trend patterns in the Pacific Ocean sea level during the altimetry era: the contribution of thermocline depth change and internal climate variability. *Ocean Dyn.* 65: 341-356. <https://doi.org/10.1007/s10236-014-0805-7>
- Royston S., Watson C.S., Legresy B., et al. 2018. Sea-level trend uncertainty with Pacific climatic variability and temporally-correlated noise. *J. Geophys. Res. Oceans* 123: 1978-1993. <https://doi.org/10.1002/2017JC013655>
- Slangen A.B.A., Church J.A., Agosta C., et al. 2016. Anthropogenic forcing dominates global mean sea-level rise since 1970. *Nat. Clim. Change* 6: 701-705. <https://doi.org/10.1038/nclimate2991>
- Stammer D., Cazenave A., Ponte R.M., et al. 2013. Causes for contemporary regional sea level changes. *Annu. Rev. Mar. Sci.* 5: 21-46. <https://doi.org/10.1146/annurev-marine-121211-172406>
- Tkalich P., Vethamony P., Luu Q.H., et al. 2013. Sea level trend and variability in the Singapore Strait. *Ocean Sci.* 9: 293-300. <https://doi.org/10.5194/os-9-293-2013>
- Vimont D.J. 2005. The contribution of the interannual ENSO cycle to the spatial pattern of decadal ENSO-like variability. *J. Clim.* 18: 2080-2092. <https://doi.org/10.1175/JCLI3365.1>
- Visser H., Dangendorf S., Petersen A.C. 2015. A review of trend models applied to sea level data with reference to the “acceleration-deceleration debate”. *J. Geophys. Res. Oceans* 120: 3873-3895. <https://doi.org/10.1002/2015JC010716>
- Widlansky M.J., Timmermann A., McGregor S., et al. 2014. An interhemispheric tropical sea level seesaw due to El Niño Taimasa. *J. Clim.* 27: 1070-1081. <https://doi.org/10.1175/JCLI-D-13-00276.1>
- Wolter K., Timlin M.S. 1998. Measuring the strength of ENSO events: how does 1997/98 rank? *Weather* 53: 315-324. <https://doi.org/10.1002/j.1477-8696.1998.tb06408.x>
- Wu Q., Luu Q.H., Tkalich P. et al. 2017. An improved empirical dynamic control system model of global mean sea level rise and surface temperature change. *Theo. Appl. Clim.* 132: 375-385. <https://doi.org/10.1007/s00704-017-2039-3>
- Zhang X., Church J.A. 2012. Sea level trends, interannual and decadal variability in the Pacific Ocean. *Geophys. Res. Lett.* 39: L21701. <https://doi.org/10.1029/2012GL053240>